Heliyon 9 (2023) e18823

Contents lists available at ScienceDirect

Heliyon

journal homepage: www.cell.com/heliyon

Modeling, simulation and performance evaluation of a PVT system for the Kenyan manufacturing sector

Veronica Ngunzi [a], Francis Njoka [a,*], Robert Kinyua [b]

[a] Department of Energy, Gas and Petroleum Engineering, Kenyatta University, P.O BOX 43844- 00100, Nairobi, Kenya
[b] Department of Physics, Jomo Kenyatta University of Agriculture and Technology, P.O. Box 62000-00200, Nairobi, Kenya

ARTICLE INFO

Keywords:
PVT module
MATLAB-Simulink simulation
Thermal energy recovery
Low-to-medium industrial heat

ABSTRACT

Manufacturing is an end-use sector that uses the most delivered energy, accounting for around 50% of all transported fuel globally and 40% of carbon dioxide emissions worldwide. Solar photovoltaic-thermal (PVT) energy can substitute the transported energy to meet thermal and electrical energy requirements, mitigating high energy costs and climatic problems. This research aimed to develop, simulate, and evaluate the capabilities of a solar photovoltaic-thermal system for potential use in Kenya's manufacturing sector. A multistage cluster sampling technique was used in the study to characterize the manufacturing industry. Additionally, a PVT system was simulated using MATLAB Simulink to ascertain the relationship of temperature and the PV electrical efficiency. The impact of incorporating a thermal collector into the PV system on electrical, thermal, and overall system efficiency, and also the system's potential for use in thermal processes in manufacturing, were assessed. From the characterization results, the agro-processing sector dominates with 35% representation, and the small-scale thermal energy category dominates at 80%. The simulation findings show that a small temperature increase leads to a small increment in short circuit current but a significant decline in open circuit voltage. As a consequence, the maximum power (Pmax) of the PV decreases, lowering its electrical efficiency. However, the integration of PV with thermal collector improved the electrical, thermal, and the entire system efficiencies by, 16.01%, 20%, and 36.13%, respectively. More than 75% of the electrical and thermal energy processes fall in the small energy category. Hence, the PVT system is suitable for small-scale low-to-medium heat thermal energy categories or as a substitute system for higher temperature processes to raise feed water temperatures and reduction of thermal energy cost. This study gives a new approach of the application of PVT system for thermal industrial applications.

1. Introduction

Environmental and/or climate protection, as well as securing dependable, affordable, and sustainable energy supply, continue to be major worldwide concerns of the twenty-first century [1]. SDG 7, which is critical to achieving the sustainable development agenda's goals of eradicating poverty, safeguarding the planet, and enhancing people's lives and prospects, is spearheaded by renewable energy technologies like solar thermal, solar photovoltaic (PV), and wind energy. Solar PV have been widely utilized to generate electricity

* Corresponding author.
E-mail address: njoka.francis@ku.ac.ke (F. Njoka).

https://doi.org/10.1016/j.heliyon.2023.e18823
Received 19 April 2023; Received in revised form 19 July 2023; Accepted 29 July 2023
Available online 6 August 2023

directly for a variety of purposes as well as integration into a wide range of industries, including hydrogen production, built-in environments, and transportation, among others [2,3]. Due to increased energy demand for cooling caused by global warming, the industrial sector is currently experiencing a rapid rise in thermal energy challenges to satisfy the thermal process energy demand as a result of competition for limited energy. Utilizing renewable energy, particularly photovoltaic-thermal (PVT) technology, can help to solve this problem [4]. A hybrid of a Photovoltaic cell and thermal collector can efficiently and affordably produce heat and electricity. Due to significant reflection or conversion of incident sunlight into deleterious thermal energy, only 5% to 25% of solar radiation can be transformed into electricity using PV technology. The PV cell's output power decreases as PV cell's temperature rises. The thermal component of the hybrid system boosts the system's overall efficiency since it works as a heat sink for the photovoltaic cells, cooling them. PVT technology has a number of intriguing residential and industrial applications. However, a number of barriers, including those in the economy, politics, law, and technology, are impeding the development of this technology. The inconsistency between the supply and demand of both heat and electricity has also hindered advancement [5]. Therefore, for the PVT technology to be adopted by major commercial markets, concerted efforts from all the main stakeholders is required [6]. The PVT technology is economically viable in industrial applications where low to high load temperatures and process heat are required [7].

Surprisingly, manufacturing processes consume more than half of total global heat demand [8]. Fossil fuels dominate in the supply of heat with little substitution from biomass and other renewables. Regardless of location, solar thermal systems offer a great potential for meeting industrial process thermal energy demand; nevertheless, due to the aforementioned limitations, adoption is rather limited [9]. Various initiatives to decarbonize the production of industrial thermal energy have been made, such as carbon capture and sequestration (CCS), electrification of industrial heat operations, and the utilization of hydrogen and biomass. The economic viability of these technologies is one of the main obstacles [10]. According to SE4ALL, (2015), industries requiring thermal energy are reportedly converting to biomass as a result of the rising cost of fuel oil. For instance, with an average annual use of 10,900 m^3 of woodfuel, or roughly 550,000 tons of woodfuel, the tea and the cottage sectors in Kenya are some of the greatest users of this fuel. Most of the woodfuel is sourced from forests and it is not sustainable because of the ever-increasing thermal energy demand exposing forests to deforestation and environmental degradation. This is replicated in various other parts of the world.

Despite the potential for industrial thermal energy supply offered by PVT technology, much research focus has been placed on small-scale integrated thermal systems for space cooling, heating and hot water supply [11–13,13,14], and research has been concentrated in other regions, particularly Asian countries [15–19]. There has been little research on industrial thermal heat applications and tropical African climatic conditions, Kenya among them.

That said, Kenya has an exceptional location close to the equator, and just like other tropical nations, it has a great solar energy resource potential. The nation enjoys year-round, good solar isolation with 4–6 kWh/m^2/day of moderate to high solar radiation. It receives 5 peak sun hours on average. The nation's overall yearly solar energy output falls between 1750 kWh and 1900 kWh for the majority of the land and varies from 700 kWh in hilly areas to 2650 kWh in dry and semi-arid areas [20]. However, just a portion of this abundant resource has been utilized thus far, mostly for lighting, heating, drying, and producing electricity [21]. Kenya's manufacturing industry is one of the country's largest most significant energy consumers [22]. According to Ref. [23], the Kenyan manufacturing sector had the highest share of energy consumption at 50.16% by 2019 with the industries of concern being pharmaceuticals, chemicals, plastics, food, clothing, and apparel. Most of the manufacturing activities are concentrated in urban commercial centers and/or city areas like Nairobi, Mombasa, Thika, and Kisumu, among others. Thermal and electrical energy from diverse sources such as woodfuel, oil, and electricity are used in these processes. Some of these energy sources are unsustainable threatening the operations of most companies and the livelihoods of many employees. The primary concern is to improve efficiency and resource management through various strategies, one of which is to incorporate renewable energy as a viable alternative energy source [24,25].

One initiative that can address the high energy costs and climate change is to consider the use of solar energy technologies, both thermal and electrical, as a replacement for conventional energies. Both technologies have symbiotic drawbacks that can be mitigated through a hybrid system that integrates the two. High cell temperatures, for example, have a substantial impact on the functioning of PV systems in hot areas [26] and roof area constraints the size of the system [27–30]. Other factors include wind energy, soiling, shading, and geographic position [31,32]. Most of the Kenyan industries lie in hot areas and PV market segment for roof top system is domineered by commercial and industrial consumers [33,34]. This provides significant potential for combined solar PVT hybrid system technology in the manufacturing sector to mitigate low efficiency caused by high temperatures and area constraints, as well as improve manufacturing industries' competitive advantage.

The fluids that are widely utilized to cool PV cells in a PVT module are air, water, and refrigerant [35]. Other examples include phase materials and nanofluids [36,37]. The working fluid is selected based on the process temperature, which ranges from low to medium to high. Water can be used across all systems because of its thermal properties, such as its high specific heat capacity, high melting point, and high boiling point [38]. The primary benefit of water-based PV/Ts is for hot water demands [39]. There have been several experimental and theoretical research studies done on these two varieties of hybrid PVT systems in the past [40]. Different researchers focused on various aspects of the system elements to realize improved efficiency and lower the costs of the overall system. An experimental study by Ref. [41] reveal that improvement of PVT collector optical attributes improved the PVT collector's overall efficiency by above 87%, with a thermal and electrical efficiency of 79% and 8.7%, correspondingly. Also, an experimental test undertaken by Ref. [42] to collate a PVT module's performance with a conventional PV, and the findings revealed that the inclusion of the thermal system increased the electrical efficiency of the PV module. The findings of the experiments also revealed that the thermal performances of PVT hybrid were superior to those of the conventional PV module and were roughly in line with those predicted theoretically. According to research by Ref. [43] who modeled and assessed the potency of an exposed PVT water collector, the overall PVT efficiency was 42% which is an improvement from 13.2% of PV. In a numerical modeling study of an exposed nanofluid sheet and

tube type PVT system [44], discovered that the utilization of pure water as a base fluid led to better outcomes than using other nanofluids. To mediate non-uniform temperature distribution in a hybrid photovoltaic (PV) thermoelectric generator (TEG) power generation system [45] examined thermal interface materials. The study, which examined the usage of three thermal interface materials in both water- and air-cooled conditions, used aluminum honeycomb cooling panels as the cooling contact material. The study revealed that employing thermal interface materials significantly reduced temperature mismatch. A PVT with combined water and air for heating was evaluated experimentally by Ref. [46] in a controlled indoor environment. The study's assumptions included an airflow rate of 0.05 kg/s, a water flow rate of 0.02 kg/s, and a radiation dose of 800 W/m^2. The system's thermal and electrical efficiency were 76% and 17%, correspondingly. Other research on cooling fluid [47,48] investigated a Nanofluid combined with phase change material and PVT with air as a cooling fluid, respectively. All these configurations showed a considerable improvement in electrical efficiency.

Among the various studies reviewed, several researchers have too used different softwares in the simulation of PVT systems. TRNSYS has been used in several studies for the simulation of domestic hot water and electricity [49–51]. Their findings showed that the combination of PV and thermal systems produced more electrical and exergy output than independent PV systems. Similar simulations in the MATLAB-Simulink environment have also been performed, with the results demonstrating increased electrical efficiency [52,53].

Following on from previous research that focused on aspects of the PVT system and domestic water application for other climates, this research focused on modeling, simulation, and performance assessment of a PVT system for industrial heat application for a tropical climate like Kenya while keeping the rooftop area constraint in mind and water as the working fluid. This was also informed by the detailed categorization of thermal processes in the Kenyan manufacturing sector that would be most useful for low and high temperature heat generated by the PVT systems.

2. Solution procedures

2.1. Characterization of the Kenyan manufacturing sector

Kenya's location close to the equator, pleasant tropical climate, and averagely high daily sunshine hours make it a country with optimal solar energy potential of 4–6 kWh/m^2/day. Given the lack of a comprehensive database on consumption of energy in the manufacturing sector, specifically thermal energy demand, the study intended to assess and characterize the thermal heat processes in

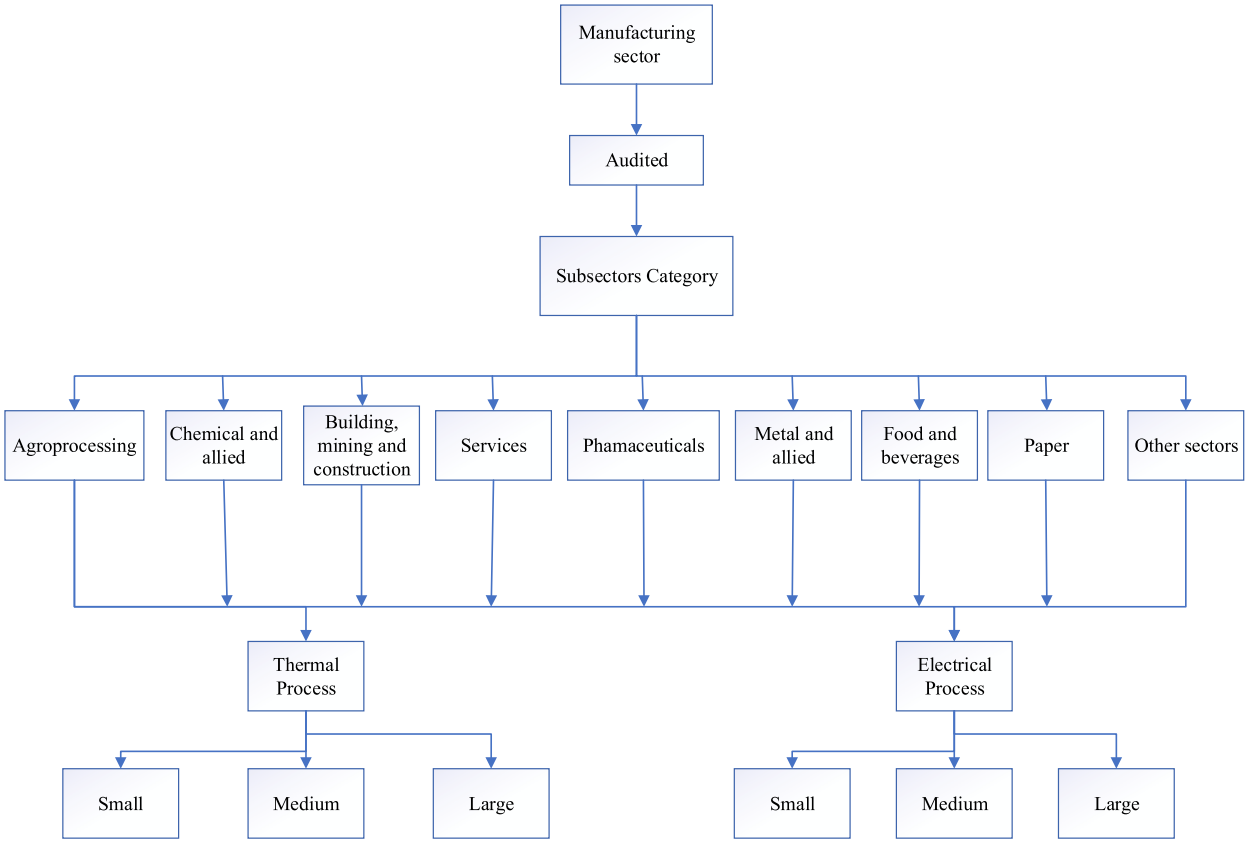

Fig. 1. Multistage cluster sampling procedures.

the entire manufacturing sector in Kenya based on all registered entities by the regulator. The national Energy and Petroleum Regulatory Authority (EPRA) provided the data for 102 registered companies that had filed Energy Audits reports for the previous year with the Authority. The study employed a multi-stage cluster sampling strategy, with the manufacturing sector serving as the population of interest for data analysis. Fig. 1 depicts the steps of cluster sampling, which included; the first stage –overall audited subsector categories, the second stage -energy processes, and the third stage -energy categorization based on the given thermal and electrical consumption metrics. More analysis was done using sigma plot version 14 as the statistical analysis tool to bring out the meaning of the data. Descriptive and regression data analysis were carried out to make inferences of the analyzed data.

2.2. Photovoltaic-thermal collector system

A PV module that absorbs incident solar irradiation is an element of the PVT system, and it is integrated with a thermal collector at the rear to absorb heat arising from transmitted (non-absorbed) radiation through the PV. An inlet flow of cold water is circulated by a solar-powered pump to cool the PV cells continuously. The thermal collector under study is a parallel flow flat plate type, and the absorbed heat is then locked up in a thermal storage tank for hot water application. The solar pump and thermostat are powered by part of the electricity produced by the system, while the remaining amount is used for other electrical applications. The system layout is depicted schematically in Fig. 2.

2.3. Numerical model for the PVT system

In simulating the dynamics of the PV panel, thermal collector, piping system, water demand, and storage tank, a set of differential equations were used to represent the PVT system. An aluminium frame, toughened cover glass, an encapsulation-polymer rear back sheet, a junction box with diodes and connectors, and solar PV cells make up the PV panel. From Fig. 3, the PV cells are made up of a current source and a diode connected in parallel. The output current, shunt current, diode reverse saturation current, reverse saturation current, and photocurrent of the PV cells were all modeled using equation 1 through 5 [54–56].

$$I = I_{ph} - I_O\left[\left[\exp\left(\frac{q(V + I * R_S)}{n * K * N_s * T}\right) - 1\right] - I_{sh}\right. \tag{1}$$

$$I_{Sh} = \frac{V + I \times R_s}{R_{sh}} \tag{2}$$

$$I_{rs} = \frac{I_{sc}}{e^{\left(\frac{q \times V_{Oc}}{n \times N_s \times K \times T}\right) - 1}} \tag{3}$$

$$I_o = I_{rs} \times \left(\frac{T}{T_n}\right)^3 \times exp\left[\frac{q \times E_{go} \times \left({}^1/_{T_n} - {}^1/_{T}\right)}{n \times K}\right] \tag{4}$$

$$I_{ph} = [I_{sc} + k_i \times (T - 298)] \times \frac{G}{1000} \tag{5}$$

Where I is the PV current output, Iph is the photo-current of the module, IO is saturation current for each module, Irs is reverse

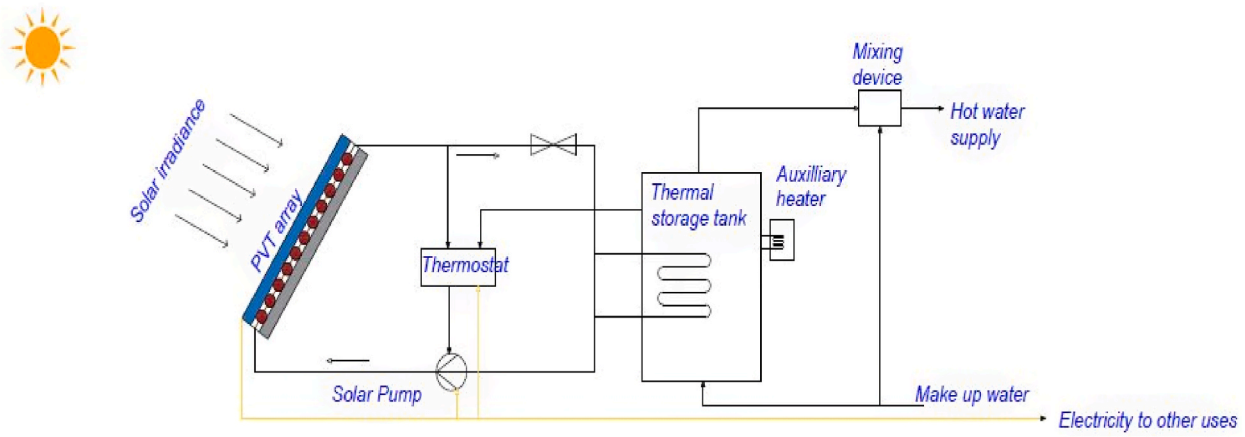

Fig. 2. Solar photovoltaic-thermal system Layout.

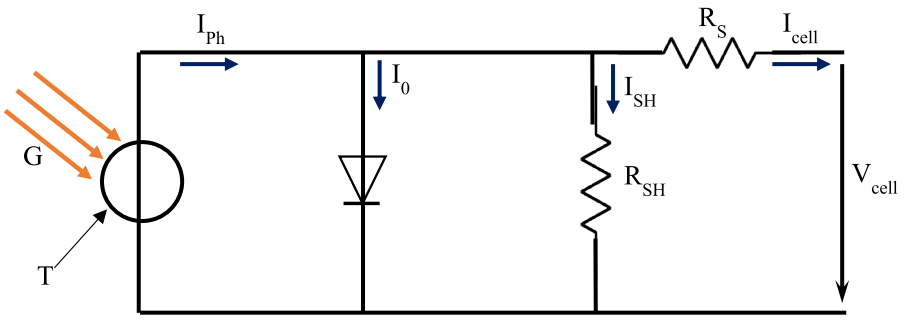

Fig. 3. A Schematic of PV cell circuit.

saturation current, Ish is the current through the shunt resistor, V is the module's terminal voltage, Voc is the open circuit voltage, RS is the diode series resistance for each module, RSh is the diode shunt resistance for each module, q is the electric charge, K is the Boltzmann constant, and n is the ideality factor of the diode for the module. T is PV cell temperature, Tn is the nominal temperature, Ego is the bandwidth of the semiconductor, G is solar radiation, ki is the short circuit current of a cell at 25 °C and 1000 W/m^2, and Ns is the number of series-connected cells.

To capture the heat produced by the PV panel, a collector absorber is positioned underneath it. Optical and energetic models were utilized to describe the thermal collector for the flat plate collector. The optimal efficiency is expressed as given in equation (6) for the optical absorption of solar radiation by the absorber, which depends on the solar incidence angle [57].

$$\eta_{opt} = \left[1 - \gamma\left(\frac{1}{cos\,\theta} - 1\right)\right] \tag{6}$$

Where η_{opt} is the optimal efficiency and γ experimental incidence angle modifier coefficient.

The energetic model using a one-dimensional model provides an acceptable precision in comparison with complex models [6]. Given its affordability and ability to achieve the highest thermal efficiency and optimal fluid temperatures, the sheet-and-tube arrangement is considered as highly potential in this modeling work [58]. In accordance with this theory, a unidimensional transient model was created by implementing energy conservation in each collector component. The model utilizes the analytic solution of the first order differential energy balance equation for the PVT collector, with the purpose to estimate heat transfer for the glass cover, PV module, absorber fin, absorber connection to the circulation tube, and fluid in the tubes, as shown in equations (7)–(11). The

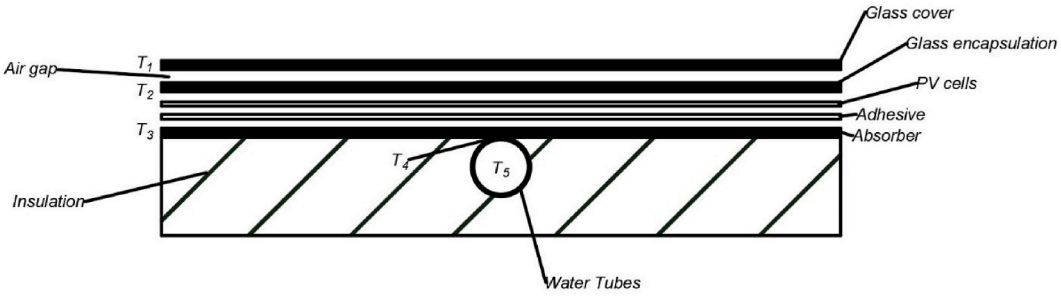

Fig. 4. Sheet-and-tube PVT collector.

$$m_1 Cp_1 \frac{dT_1}{dt} = C_{11}(T_1 - T_{amb}) + C_{12}\left(T_1^4 - T_{sky}^4\right) + C_{13}(T_2 - T_1) \tag{7}$$

$$m_2 Cp_2 \frac{dT_2}{dt} = C_{21}G + C_{22}(T_2 - T_1) + C_{23}\left(T_2^4 - T_1^4\right) - C_{24}\eta_e G - C_{25}(T_2 - T_3) - C_{25}(T_2 - T_4) \tag{8}$$

$$m_3 Cp_3 \frac{dT_3}{dt} = C_{31}(T_2 - T_3) + C_{32}\left(T_3^4 - T_{amb}\right) + C_{33}\left(T_4 - \frac{K_1 T_2 + K_2 T_{amb}}{K_3}\right) \tag{9}$$

$$m_4 Cp_4 \frac{dT_4}{dt} = C_{41}(T_2 - T_4) + C_{42}(T_4 - T_5) + C_{33}\left(T_4 - \frac{K_1 T_2 + K_2 T_{amb}}{K_3}\right) \tag{10}$$

$$m_5 Cp_5 \frac{dT_5}{dt} = C_{51}(T_4 - T_5) + C_{42}(T_4 - T_5) \tag{11}$$

position of temperatures Ti are shown in Fig. 4.where m represents mass, C_p is the specific heat capacity, T is temperature, η_e is electrical efficiency.

T_5 shows the fluid medium's temperature as calculated in equation (12);

$$T_5 = \frac{T_{out} + T_{in}}{2} \tag{12}$$

The calculations are simplified using the constants C_{ij} and K_i, which are non-temperature related attributes derived from the geometrical values of the collector, optical characteristics, and heat transfer coefficients. The PVT module's electrical and thermal efficiency are calculated by Equations (13) and (14), respectively.

$$\eta_e = \eta_{cel}\tau_g \tag{13}$$

Table 1
Specifications of the model input parameters.

Parameter	Value
Load Resistance (ohm)	4.5
PVT properties	
Glass cover, PV cells, back cover initial temperature [K]	298.15
Area of a PV cell (m^2)	0.02755
Number of cells	72
Refractive index ratio glass/air	1.52
Absorption coefficient of glass per unit length	0.3
Glass cover thickness [m]	0.003
Reflection factor of PV cell (85% is absorbed)	0.15
Glass cover mass [kg]	4
PV cell mass [kg]	0.2
Heat exchanger mass of [kg]	15
Back cover mass [kg]	5
Glass Specific heat [J/kg/K]	840
PV cell Specific heat [J/kg/K]	700
Heat of heat exchanger Specific heat [J/kg/K](copper)	387
Back cover Specific heat [J/kg/K]	400
Glass Emissivity	0.89
PV cell Emissivity	0.75
Free convection coefficient between glass and ambient air [$W/m^2/K$]	10
Free convection coefficient between back cover and ambient air [$W/m^2/K$]	10
Heat exchanger thermal conductivity [W/m/K]	386
Heat exchanger thickness [m]	0.04
Insulation layer thermal conductivity [W/m/K]	0.1
Insulation layer thickness of [m]	0.03
Short-circuit current, Isc [A]	8.89
Open-circuit voltage, Voc [V]	45
Diode saturation current, Is [A]	1e-6
Diode saturation current, Is2 [A]	0
Solar-generated current for measurements, Iph [A]	8.89
Reference irradiance, Ir [W/mˆ2]	1000
Diode ideality factor	1.5
Series resistance, Rs [Ohm]	0.221
Energy gap, EG [eV]	1.1
Measurement temperature [°C]	25
Pipe and tank parameters	
Pipe length (m)	4
Cross sectional area (m^2)	0.00005
Hydraulic diameter (m)	0.03
Internal surface absolute roughness [m]	15e-6
upper Reynolds number limit for laminar flow	2500
Lower Reynolds number limit for turbulent flow	3900
Nusselt number for laminar flow heat transfer	3.66
Maximum tank capacity [m^3]	0.5
Tank cross-sectional area [m^2]	0.6
Initial Tank capacity [m^3]	0.1
Initial tank temperature [K]	295.15
Insulating layer thickness [m]	0.05
Insulation layer thermal conductivity of [W/m/K]	0.1
Free convection coefficient between tank and ambient air [$W/m^2/K$]	10
Internal circuit mass flow rate [kg/s]	0.02
Consumption mass flow rate (to the sink) [kg/s]	0.005
Source mass flow rate (from the source) [kg/s]	0.005

$$\eta_t = \frac{mC_p\left(T_{fout} - T_{fin}\right)}{G} \tag{14}$$

Where η_{ce} is the photovoltaic cells efficiency, η_t is the thermal efficiency, τ_g is the transmittance of the glass cover, T_{fout} is the temperature of the fluid in, and T_{fin} is the temperature of the fluid out. Thermal storage tank with constant pressurization and variable fluid volume is used in the model. Heat transfer takes place by means of convection when liquid flows into or out of the enclosure, and conduction when thermal energy passes through the liquid at the tank's inlets and the tank's wall. The total fluid mass at each time step is used to calculate the tank's fluid volume as shown in equation (15).

$$V = \frac{m}{\rho} \tag{15}$$

Equations (16) to 18) illustrate how the conservation equation is used to model the balance of mass, momentum, and energy.

$$\dot{m} = \dot{m}_A \tag{16}$$

$$\rho_A = \rho_{dyn} = \rho P_{Ref} + \rho(y - y_A) \tag{17}$$

$$m\left(C_p - h\beta\right)T = \Phi_A - \dot{m}_A h + Q \tag{18}$$

Where $\dot{m}$ net mass flow rate into the tank, $\dot{m}_A$ is the mass flow rate into the tank fluid volume through the inlet is ρ_A Liquid density at inlet, y is the tank level, or height, relative to the tank bottom, y_A is the tank inlet elevation relative to the tank bottom β is the Fluid isobaric bulk modulus, ΦA is the energy flow rate into the tank through inlet, h Fluid enthalpy and Q is the thermal energy flow rate into the tank through output port. The pump is modeled using The Controlled Mass Flow Rate Source (TL) and pipe flow dynamics from the Simscape fluids. The water demand, pump, and piping are modeled based on the user demand rate, source supply rate, and inner flow that propels convection in the pipe. The parameters used for modeling are shown in Table 1.

2.4. Simulation procedures

Utilizing the governing equations, MATLAB-Simulink simulation tool was applied in the simulation of the electrical power of the PVT system and heat cogeneration utilizing a hybrid PVT solar module. Irradiance was varied to demonstrate its impact on the system's overall performance, solar cell temperature, and both electrical and thermal power. While the heat created was transmitted to the water for thermal energy consumption, the generated electricity was used to power the electrical load i.e. the pump and other applications. Simscape Fluids™ libraries provided component libraries to model and simulate the thermal portion of the panel. On the other hand, Simscape Electrical™ libraries provided component libraries for the electronic, mechatronic, and electrical power systems to evaluate the generation, conversion, transmission, and utilization of electrical power. The PV cells in the electrical portion of the network were simulated by a solar cell block, and a resistive load was simulated by a load sub-system. The heat transfer between the PV panel's components, including the glass cover, PV cells, absorber, back cover, and surroundings, was simulated using a thermal network. The heat was transferred by radiation, convection, and conduction. The heat exchangers, tank, and pipe made up the thermal-

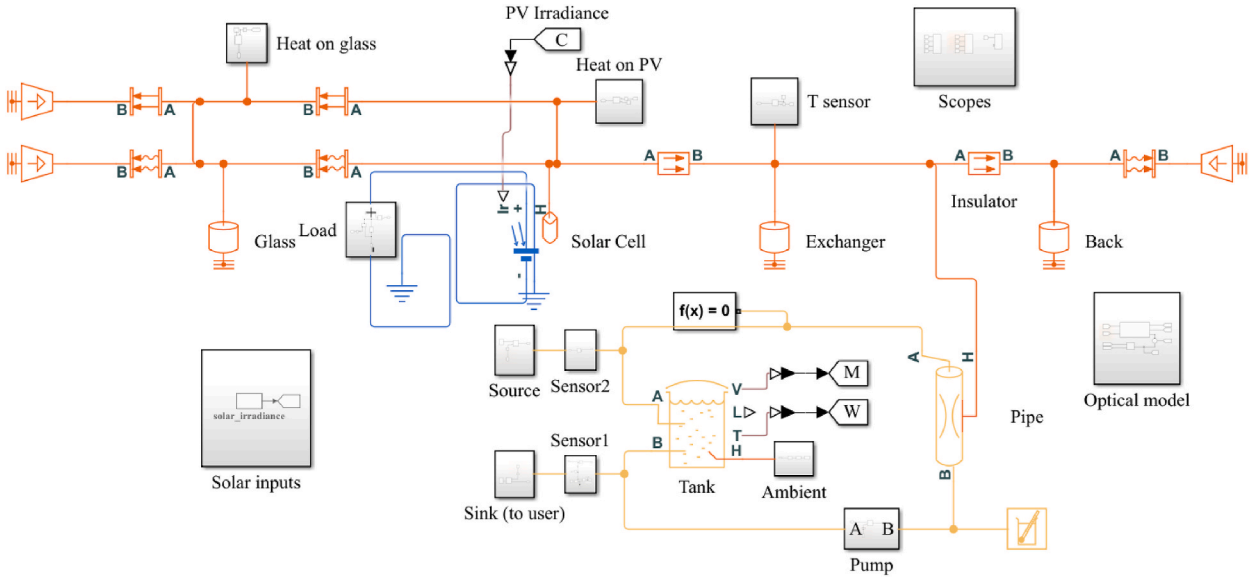

Fig. 5. Simulation model layout.

liquid network. Simulink was utilized to help with system design, simulation, automatic code generation, and continuous testing and verification. The simulation was run during the time of solar insolation. Fig. 5 depicts the simulation used in this investigation.

2.5. Model validation

Model validation was performed for consistency testing with an experimental evaluation of a PVT system with similar characteristics. The relationship of irradiance and water temperature for the simulation was validated against researches of [59–62]. The relationship of irradiance and solar cell temperature was validated against [61]. Additionally, the overall, thermal, and electrical efficiency of the system was compared with other authors' systems.

2.6. Assumptions

During model setup and simulation procedures, several assumptions were made which included; quasi-steady state system, uniform temperature across each PVT lamina, negligible heat loss and pressure drop in the system, and a uniform wind speed surrounding the system.

3. Results and discussion

3.1. Characteristics of Kenya's manufacturing sector

3.1.1. Sector categories

One hundred and two (102) audited facilities with both thermal and electrical systems, representing 11% of the facilities in Kenya's manufacturing sector were examined. It is a requirement by the Kenyan government for facilities consuming more than 680 GJ of energy to conduct energy audit by licensed auditor every three years. According to Ref. [63], just 43% of the specified facilities' entire population has had energy audits carried. According to the report, hurdles to low compliance include a lack of funding to conduct energy audits, competing budget interests with other activities at facilities, a limited number of licensed energy auditors, and a general lack of awareness of energy management systems. The 11% satisfied the require statistical sample size. The distribution of the sectors is presented in Fig. 6, with the agro-processing sector representing the highest number of audited facilities at 35.3% and the automotive sector with the lowest number of facilities at 1%.

3.1.2. The electrical and thermal energy shares

Electrical and thermal energy categorization was based on metrics obtained from Kenya association of manufacturers as indicated in Table 2. The energy consumption by various end use processes by sectors was categorized into small, medium and large energy consumers in the electrical and thermal sub-categories as illustrated in Fig. 7(a) and (b), respectively. The small sector category for both electrical and thermal were largely represented at 29.4% and 19.6%, respectively. Fig. 7(b) also shows the general categorization of the thermal energy sector where the small thermal energy categorization domineered the industry at 78.4%. The thermal energy categorization was of interest in the evaluation of the possible applications of the PVT technology in the manufacturing sector.

3.1.3. Thermal energy category

The thermal energy category is further studied to establish the most suitable application areas for the PVT. The agro-processing, service, food and beverage, and metal and allied were further studied and compared to the overall share of each category since

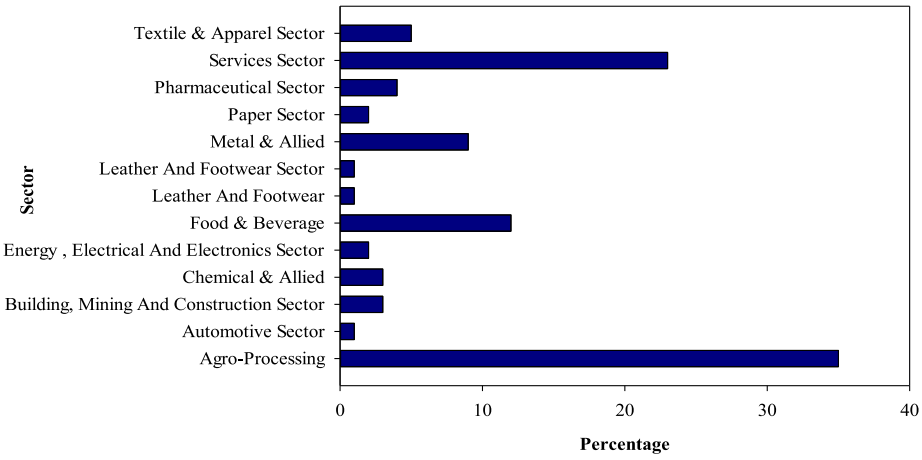

Fig. 6. Audited manufacturing sector representation.

Table 2
Energy Consumption Metrics as defined by EPRA.

Category	Electrical Energy Consumption		Thermal Energy Consumption	
	Lower Limit (GJ)	Upper Limit (GJ)	Lower Limit (GJ)	Upper Limit (GJ)
Small Consumers	0	15000	0	45000
Medium Consumers	15000	45000	45000	135000
Large Consumers	45000	No limit	135000	No limit

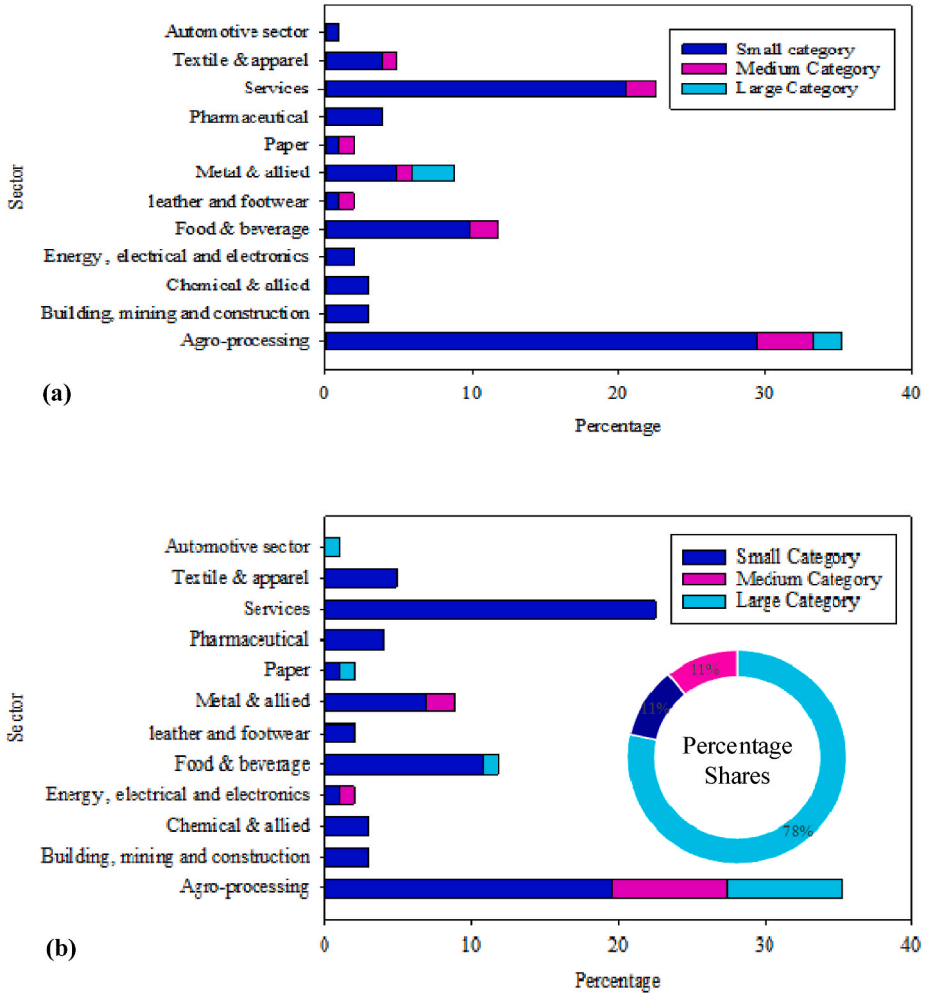

Fig. 7. Energy categorization; (a) Electrical distribution and (b) Thermal distribution.

they domineered the small thermal energy category as shown in Fig. 8. The agro-processing sector dominated the small thermal energy category at 19.6% and the service sector at 18.62%. The agro-processing sector dominated the medium thermal energy category at 7.8%, followed by metal and allied at 2.94%. The tea and floriculture industries dominated agro-processing. In the tea processing industry, thermal energy is required to generate steam at 180 °C. As a result, this system could be used to pre-heat water. Hot water is required in the floriculture sector for propagation and soil treatment at 18–30 °C and above 49 °C, respectively. Banks and hotels with hot temperature requirements above 40 °C dominated the service industry.

3.1.4. thermal energy consumption categories

Fig. 9(a), (b), and (c) depict the energy consumption of facilities in the small, medium, and large thermal energy categories, respectively. In the small thermal energy category, 63% of the facilities consumed less than 2,500 GJ of thermal energy, while 72.7% of the medium thermal energy category facilities consumed less than 90,000 GJ of thermal energy. Further to that, 72.7% of facilities in the large thermal energy category consumed less than 290,000 GJ of thermal energy.

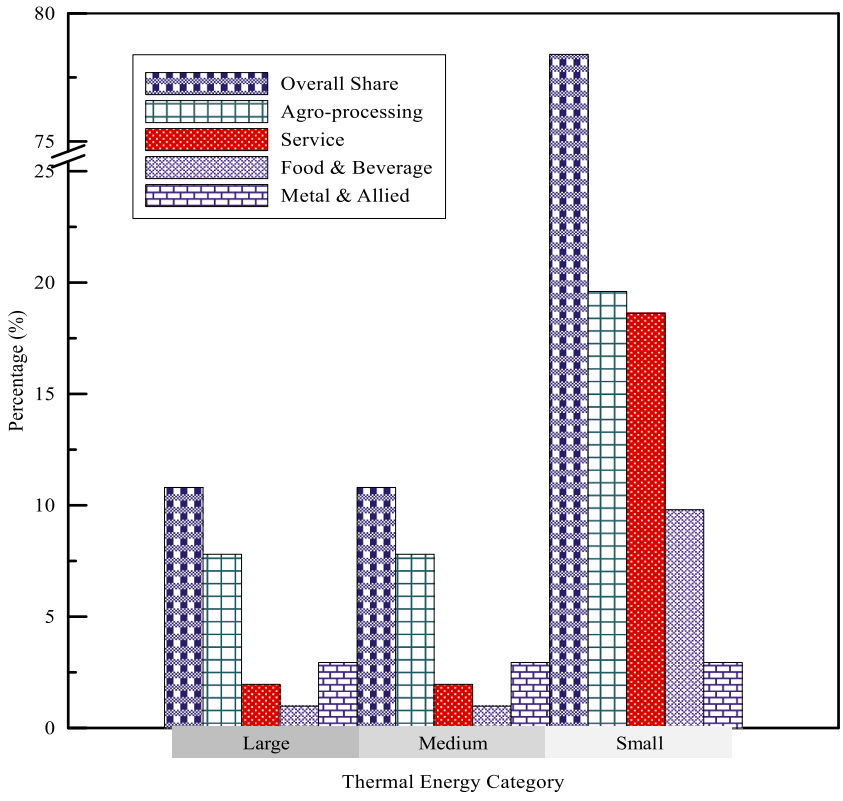

Fig. 8. Comparison of thermal energy categorization.

3.2. Irradiance and PV output characteristics

Fig. 10 shows the simulation results for irradiance during solar insolation in a day. The highest simulated irradiance was at 1400 h, which was 1000 W/m^2, and this was the time of the highest insolation.

The I–V and *P*–V behavior of a 72 cell, 300 W PV module are shown in Fig. 11(a) and (b) at various temperatures. Although the open-circuit voltage significantly drops as the temperature rises, the short-circuit current rises marginally. Hence, the maximum power (Pmax) of the PV reduces, which lowers its electrical efficiency. The purpose of this experiment was to compare the actual curves to the simulated curves and ensure that the model was properly functioning.

3.3. Validation Results

The experimental data that was readily available was for irradiance and temperature. There is, however, a correlation between irradiance, solar cell temperature, and water temperature. Increased irradiance raises solar cell's the temperature, which raises the temperature of the water. As a result, a regression analysis was performed to compare simulated and experimental data from other authors for irradiance against solar cell temperature and water temperature in order to investigate experimental system performance and validate the simulation. Despite other conditions that may affect system performance, such as weather, an increase in irradiance led to increases in solar cell temperature and water temperature. The regression analysis is shown in Fig. 12(a) and (b). Again, the data available only gave the average efficiencies for electrical, thermal and overall which were validated with the average simulated data. The system's average electrical, thermal, and overall efficiencies predicted by the simulation were 16.01%, 20%, and 36.13%, respectively. The comparison is as shown in Fig. 12(c). The simulation findings matched the aforementioned studies where the overall efficiency of the systems increased by between 10 and 17%.

3.4. Simulated PVT component temperatures, power, and irradiance

The simulated temperatures for the solar cell, the back, the exchanger, the glass cover, and the water are presented in Fig. 13(a). The temperature increased with irradiance. The highest solar cell temperature was about 322 K (47.85 °C), while the highest water temperature was 317 K (43.85 °C). The highest glass temperature is 307.95 K (34.8 °C), while the highest back temperature was 301.75 K (28.6 °C). Comparing the temperatures and irradiance, the highest temperatures for the components correspond to the highest irradiance simulated, which was 1000 W/m^2. Since the model was transient the temperature were low compared to other

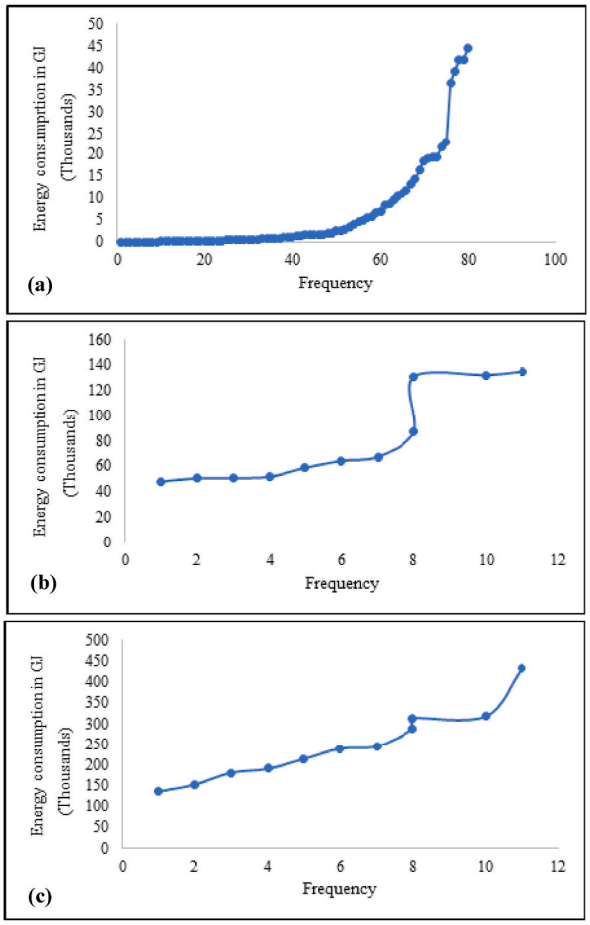

Fig. 9. Thermal energy consumption categorization: (a) Small category, (b) medium category, and (c) large category.

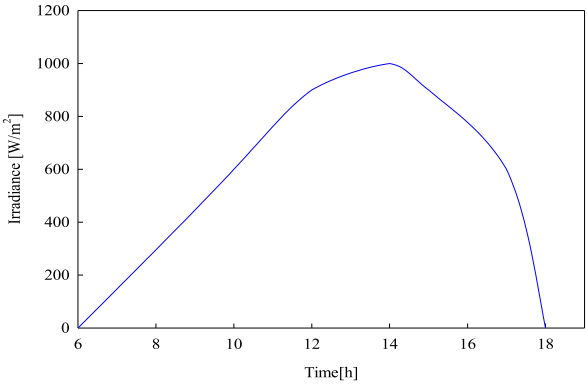

Fig. 10. Simulated irradiance.

studies. On the other hand, the simulated electrical power to the load, thermal power to water, and PV-generated electrical power are represented in Fig. 13(b). The highest electrical energy to the load, thermal energy to water, and PV electrical energy generated are 254 W, 438 W, and 1606 W, respectively. In proportion to the rise in irradiance, the electrical energy increased. The thermal energy continued to increase even with increased radiation, and then started to drop with decreased radiation.

The relationship between solar temperature and irradiance was calculated through a regression analysis of the simulation results and shown in equation (19) and Table 3(a) with R^2 of 0.864 explaining that irradiance affects solar cell temperature at 86.4% while other factors that were not considered in this study accounting for 13.6%. Similarly, the relationship between water temperature and

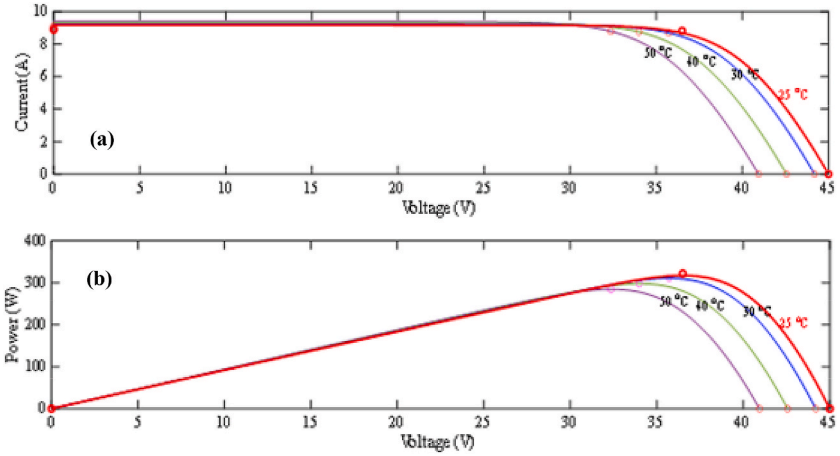

Fig. 11. Characteristics of a 72-cell, 300-W module: (a) I–V curve (b) *P*–V curve.

solar cell temperature is shown in equation (20) and Table 3(b), with an R^2 of 0.603 where water temperature is affected by solar cell temperature at 60.3%.

$$\text{Solar cell temperature} = (0.0249 \times \text{Irradiance}) + 296.107 \tag{19}$$

$$\text{Water temperature} = (0.572 \times \text{Solar cell temperature}) + 127.084 \tag{20}$$

The highest water temperature achieved was 43.85 °C. Particularly in the small thermal energy category for agro-processing, metal & allied industries, food & beverage and service sectors, the thermal heat generated by cooling the PV can be utilized to substitute for the thermal energy demand for temperatures between 18 °C and 180 °C. This can be achieved when the heat from the PVT system is used to energize a refrigerant for heat driven refrigeration cycles and heat pumps for industrial systems with refrigerant temperature ranges between 25 °C and 50 °C.

4. Conclusion

From the study, thermal energy processes in the Kenyan manufacturing sector were characterized as low, medium, and large thermal energy consumers. The small thermal energy category dominated the industry at 78.4%, and the agro-processing sector dominated the small thermal energy category at 19.6%. In the small thermal energy category, 63% of the facilities consumed less than 2,500 GJ of thermal energy where tea and coffee took the lead, followed by floriculture and fresh produce sectors while 72.7% of the medium thermal energy category facilities consumed less than 90,000 GJ of thermal energy domineered by tea and coffee sector. Furthermore, 72.7% of the facilities in the large thermal energy category consumed less than 290,000 GJ of thermal energy. Overall, over 75% of the facilities were in the small thermal energy category and consumed less than 40,000 GJ of thermal energy. Integrating a PV and thermal collector in the same module cools the PV cells, improving the module's efficiency. From the simulation results, the combined efficiency increased from 16.01% to 36.13%. This is consistent with other researchers' results that higher irradiance causes an increase in solar cell temperature, and cooling causes an increase in efficiency, which other researchers estimate to be between 10% and 17%.This system is ecofriendly and secure hence reducing global warming and climate change. The integrated PVT hybrid system has the potential to be used especially in the small energy thermal and electrical category since they constitute over three quarters of thermal energy processes in Kenya's manufacturing industries. When it comes to thermal energy, agro-processing is the most significant manufacturing industry, and the tea and coffee industries dominate this subsector. Future studies could be done to evaluate a specific thermal energy category and compare different working fluids.

Author contribution statement

Veronica Ngunzi: Conceived and designed the experiments; Performed the experiments; Analyzed and interpreted the data; Contributed, materials and analysis data; Wrote the paper.

Francis Njoka: Conceived and designed the experiments; Analyzed and interpreted the data; Wrote the paper.

Robert Kinyua: Analyzed and interpreted the data; Contributed, materials and analysis data; Wrote the paper. new.

Data availability statement

Data will be made available on request.

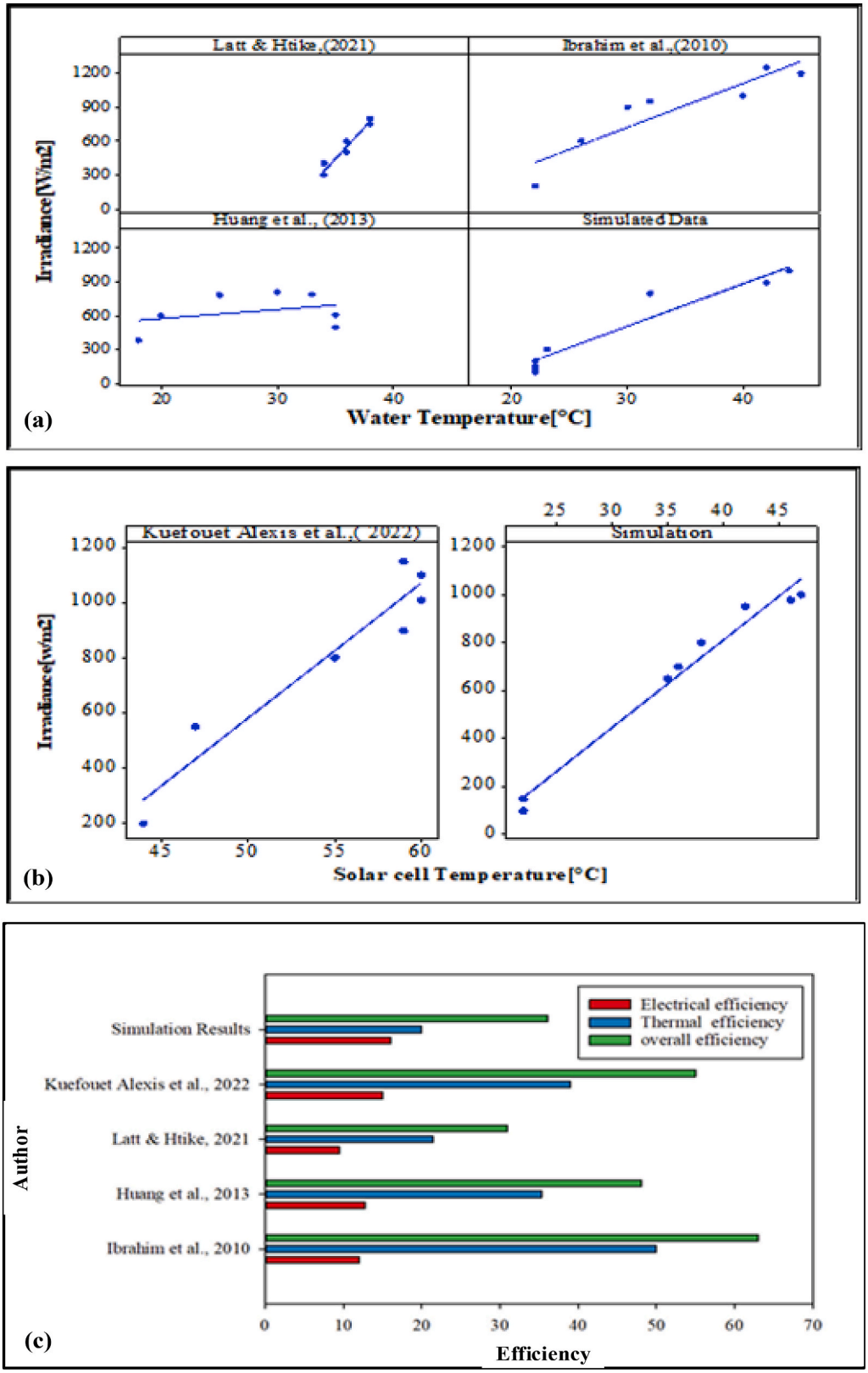

Fig. 12. Validation results: (a) Irradiance and water temperature; (b) irradiance and solar cell temperature; and (c) electrical, thermal, and overall efficiency.

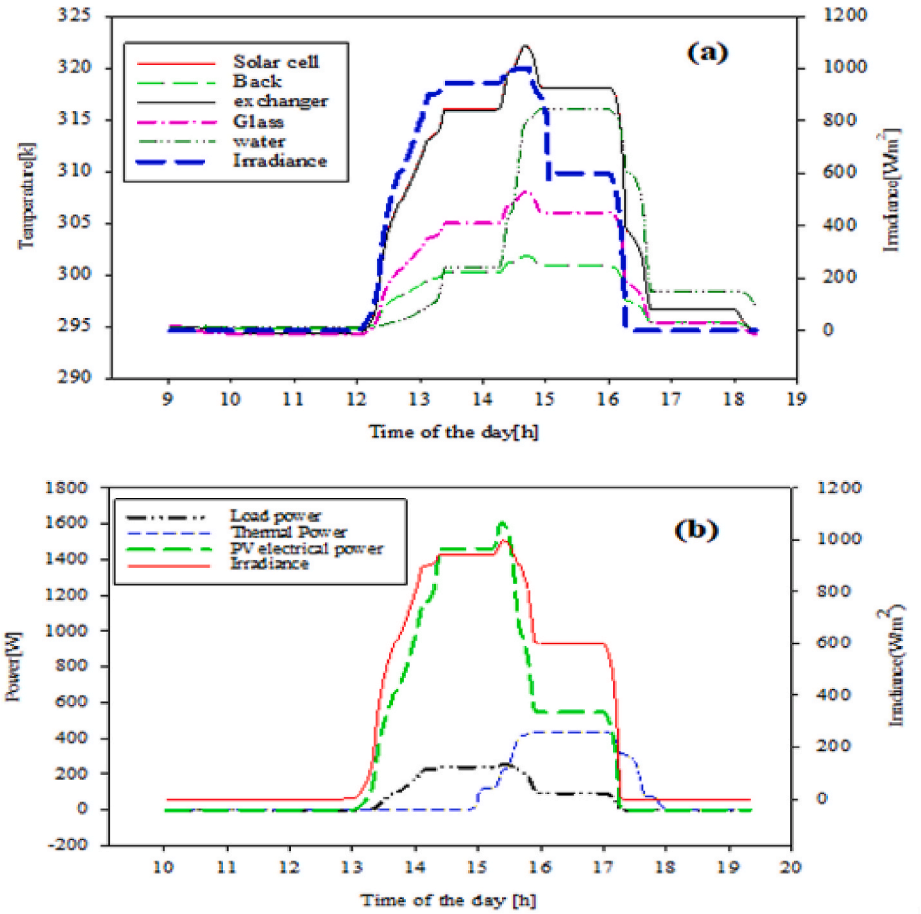

Fig. 13. Simulation of; (a) PVT Component Temperatures and irradiance (b) Power and Irradiance.

Table 3
Regression Analysis; (a) Solar cell Temperature on irradiance and (b) Water temperature on solar cell Temperature.

(a)			
Goodness of fit	Test statistics	P value	
Adjusted R-Squared	0.864		
R-Squared	0.864		
F-Statistic	2960.637	<0.001	
Dependent Variable=Solar cell temperature		Linear Regression Results	
		t-statistic	***P*-value**
Constant	296.107	1301.906	<0.001
Irradiance	0.0249		<0.001
(b)			
Goodness of fit	Test statistics	P value	
Adjusted R-Squared	0.602		
R-Squared	0.603		
F-Statistic	707.041	<0.001	
Dependent Variable= Water temperature		**Linear Regression Results**	
	Coefficients	**t-statistic**	***P*-value**
Constant	127.084	19.436	<0.001
Solar cell temperature	0.572	26.59	<0.001

Declaration of competing interest

The authors declare that they have no known competing financial interests or personal relationships that could have appeared to influence the work reported in this paper.

Acknowledgments

The authors of this work are grateful to Kenyatta University for financial support to VN as her PhD study tuition (Ref: J98/26980/2018) and to carry out this work. The authors also wish to express their gratitude to the Kenya Association of Manufacturers (KAM) and the Energy and Petroleum Regulatory Authority (EPRA) for providing the necessary data.

Nomenclature

α	Photovoltaic module absorptance
ρ_d	Reflectance associated with diffuse radiation
A	Collector area, m^2
C_p	The fluid thermal capacity
C_{pi}	Specific heat of collector components, J kg^{-1} K^{-1}
G	Solar irradiance, Wm^{-2}
g	Gravitational constant
h	Fluid enthalpy
I	Output current
I_o	Saturation current
I_{ph}	Photo current, A
I_{rs}	Reverse saturation current
I_{sc}	short circuit current
I_{sh}	Current through the shunt resistor
K	Boltzmann's constant
k_i	short circuit current of a cell at 25 °C, 1000 W/m^2
m	Tank fluid mass.(kg)
$\dot{m}$	Net mass flow rate into the tank
$\dot{m}_A$	Mass flow rate into the tank fluid volume through the inlet.
m_i	Mass of collector components, kg
N_s	Number of cells connected in series
q	electron charge, (C)
Q	Thermal energy flow rate into the tank through output port
R_s	series resistance, (Ω)
R_{sh}	Shunt resistance, (Ω)
T	Operating Temperature, K
T	Fluid temperature
T_1	Glass cover temperature of, K
T_2	PV module Temperature, K
T_3	Absorber fin Temperature of, K
T_4	Temperature of absorber fin connection to tube,K
T_5	Circulating water average temperature of, K
Tf_{in}	temperature of fluid inlet, K
Tf_{out}	Temperature fluid outlet, K
T_n	Nominal Temperature, K
T_{sky}	Sky temperature, K
V	Tank fluid volume(m^3)
V_{oc}	Open circuit voltage, (V)
y	The tank level, or height, relative to the tank bottom
y_A	The tank inlet elevation relative to the tank bottom
β	Fluid isobaric bulk modulus
η_{cel}	Photovoltaic cells efficiency
η_e	Electric efficiency
ρ	Tank fluid density
ρ_A	Liquid density at inlet
τ_g	Glass cover transmittance
τ_a	Transmittance–absorptance product
Φ_A	Energy flow rate into the tank through inlet

References

[1] IRENA, Climate Change and Renewable Energy: National Policies and the Role of Communities, Cities and Regions (Report to the G20 Climate Sustainability Working Group (CSWG)), International Renewable Energy Agency, Abu Dhabi.," Abu Dhabi, Jun. 2019.

[2] M. Aghaei, H. Ebadi, A.K.V. de Oliveira, S. Vaezi, A. Eskandari, J.M. Castañón, New concepts and applications of solar PV systems, in: Photovoltaic Solar Energy Conversion, Elsevier, 2020, pp. 349–390, https://doi.org/10.1016/B978-0-12-819610-6.00011-9.

[3] S. Senthilraja, R. Gangadevi, H. Köten, R. Marimuthu, Performance assessment of a solar powered hydrogen production system and its ANFIS model, Heliyon 6 (10) (Oct. 2020), e05271, https://doi.org/10.1016/j.heliyon.2020.e05271.

[4] K. Mostakim, M. Hasanuzzaman, Global prospects, challenges and progress of photovoltaic thermal system, Sustain. Energy Technol. Assessments 53 (Oct. 2022), 102426, https://doi.org/10.1016/j.seta.2022.102426.

[5] D.O. Cabral, Photovoltaic-thermal solar collectors – a rising solar technology for an urban sustainable development, in: Urban Transition - Perspectives on Urban Systems and Environments [Working Title], IntechOpen, 2022, https://doi.org/10.5772/intechopen.104543.

[6] H.A. Zondag, et al., "PVT Roadmap. A European Guide For The Development And Market Introduction Of PVT Technology," Netherlands, Technical Report ECN-RX-05-170, Nov, 2005.

[7] S.A. Kalogirou, Y. Tripanagnostopoulos, Industrial application of PV/T solar energy systems, Appl. Therm. Eng. 27 (8–9) (Jun. 2007) 1259–1270, https://doi.org/10.1016/j.applthermaleng.2006.11.003.

[8] Intergovernmental Panel on Climate Change, Climate Change 2014: Mitigation of Climate Change: Working Group III Contribution to the IPCC Fifth Assessment Report, first ed., Cambridge University Press, 2015 https://doi.org/10.1017/CBO9781107415416.

[9] IRENA and IEA-ETSAP, "Solar Heat for Industrial Processes," Technology Brief, Jan, 2015 [Online]. Available: www.irena.org/Publications.

[10] O. Olsson, F. Schipfer, "Decarbonizing Industrial Process Heat: The Role Of Biomass," Research Report 978-1-910154-96–0 [Online]. Available:, 2021 http://hdl.handle.net/20.500.12708/40451.

[11] A.H.A. Al-Waeli, H.A. Kazem, M.T. Chaichan, K. Sopian, A review of photovoltaic thermal systems: achievements and applications, Int. J. Energy Res. 45 (2) (Feb. 2021) 1269–1308, https://doi.org/10.1002/er.5872.

[12] S. Diwania, S. Agrawal, A.S. Siddiqui, S. Singh, Photovoltaic–thermal (PV/T) technology: a comprehensive review on applications and its advancement, Int. J. Energy Environ. Eng. 11 (1) (Mar. 2020) 33–54, https://doi.org/10.1007/s40095-019-00327-y.

[13] A. Riaz, R. Liang, C. Zhou, J. Zhang, A review on the application of photovoltaic thermal systems for building façades, Build. Serv. Eng. Technol. 41 (1) (Jan. 2020) 86–107, https://doi.org/10.1177/0143624419845117.

[14] M. Tripathy, P.K. Sadhu, S.K. Panda, A critical review on building integrated photovoltaic products and their applications, Renew. Sustain. Energy Rev. 61 (Aug. 2016) 451–465, https://doi.org/10.1016/j.rser.2016.04.008.

[15] A.H.A. Al-Waeli, K. Sopian, M.T. Chaichan, H.A. Kazem, H.A. Hasan, A.N. Al-Shamani, An experimental investigation of SiC nanofluid as a base-fluid for a photovoltaic thermal PV/T system, Energy Convers. Manag. 142 (Jun. 2017) 547–558, https://doi.org/10.1016/j.enconman.2017.03.076.

[16] N. Choubineh, H. Jannesari, A. Kasaeian, Experimental study of the effect of using phase change materials on the performance of an air-cooled photovoltaic system, Renew. Sustain. Energy Rev. 101 (Mar. 2019) 103–111, https://doi.org/10.1016/j.rser.2018.11.001.

[17] J.-H. Kim, J.-T. Kim, The experimental performance of an unglazed PVT collector with two different absorber types, Int. J. Photoenergy (2012) 1–6, https://doi.org/10.1155/2012/312168, 2012.

[18] N. Xu, J. Ji, W. Sun, W. Huang, Z. Jin, Electrical and thermal performance analysis for a highly concentrating photovoltaic/thermal system, Int. J. Photoenergy (2015) 1–10, https://doi.org/10.1155/2015/537538, 2015.

[19] B. Zhang, J. Lv, H. Yang, T. Li, S. Ren, Performance analysis of a heat pipe PV/T system with different circulation tank capacities, Appl. Therm. Eng. 87 (Aug. 2015) 89–97, https://doi.org/10.1016/j.applthermaleng.2015.04.074.

[20] M. Takase, R. Kipkoech, P.K. Essandoh, A comprehensive review of energy scenario and sustainable energy in Kenya, Fuel Commun. 7 (Jun. 2021), 100015, https://doi.org/10.1016/j.jfueco.2021.100015.

[21] J.K. Kiplagat, R.Z. Wang, T.X. Li, Renewable energy in Kenya: resource potential and status of exploitation, Renew. Sustain. Energy Rev. 15 (6) (Aug. 2011) 2960–2973, https://doi.org/10.1016/j.rser.2011.03.023.

[22] S.M. Onuonga, M. Etyang, G. Mwabu, "The demand for energy in the Kenyan manufacturing sector,", J. Energy Dev. 34 (1/2) (2008) 265–276.

[23] K.K. Macharia, J.K. Gathiaka, D. Ngui, "Energy efficiency in the Kenyan manufacturing sector,", Energy Pol. 161 (2022), 112715 https://doi.org/10.1016/j.enpol.2021.112715. Feb.

[24] O. Joash, P. Mercy, "Promoting The use Of Solar Energy In The Manufacturing Sector In Kenya," Promoting The Use Of Solar Energy In The Manufacturing Sector In Kenya, Oct. 27, 2022.

[25] I.J. Mwenda, "Analysis of Energy Utilization and Renewable Energy Potential in KTDA Region Two Tea Factories in Kenya," Master of Science Thesis, Jomo Kenyatta University of Agriculture and Technology, Kenya, 2016.

[26] S. Dubey, J.N. Sarvaiya, B. Seshadri, Temperature dependent photovoltaic (PV) efficiency and its effect on PV production in the world – a review, Energy Proc. 33 (2013) 311–321, https://doi.org/10.1016/j.egypro.2013.05.072.

[27] J. Byrne, J. Taminiau, L. Kurdgelashvili, K.N. Kim, A review of the solar city concept and methods to assess rooftop solar electric potential, with an illustrative application to the city of Seoul, Renew. Sustain. Energy Rev. 41 (Jan. 2015) 830–844, https://doi.org/10.1016/j.rser.2014.08.023.

[28] G. Desthieux, et al., Solar energy potential assessment on rooftops and facades in large built environments based on LiDAR data, image processing, and cloud computing. Methodological background, application, and validation in geneva (solar cadaster), Front. Built Environ. 4 (2018) 14, https://doi.org/10.3389/fbuil.2018.00014. Mar.

[29] S. Izquierdo, M. Rodrigues, N. Fueyo, A method for estimating the geographical distribution of the available roof surface area for large-scale photovoltaic energy-potential evaluations, Sol. Energy 82 (10) (Oct. 2008) 929–939, https://doi.org/10.1016/j.solener.2008.03.007.

[30] K. Mainzer, S. Killinger, R. McKenna, W. Fichtner, Assessment of rooftop photovoltaic potentials at the urban level using publicly available geodata and image recognition techniques, Sol. Energy 155 (Oct. 2017) 561–573, https://doi.org/10.1016/j.solener.2017.06.065.

[31] D. Cura, M. Yilmaz, H. Koten, S. Senthilraja, M.M. Awad, Evaluation of the technical and economic aspects of solar photovoltaic plants under different climate conditions and feed-in tariff, Sustain. Cities Soc. 80 (May 2022), 103804, https://doi.org/10.1016/j.scs.2022.103804.

[32] S.M. Ngure, A.B. Makokha, E.O. Ataro, M.S. Adaramola, Degradation analysis of Solar photovoltaic module under warm semiarid and tropical savanna climatic conditions of East Africa, Int. J. Energy Environ. Eng. 13 (2) (2022) 431–447, https://doi.org/10.1007/s40095-021-00454-5. Jun.

[33] P. Bhamidipati, H. Njoroge, L. Strange, M.B. Pedersen, I. Nygaard, U.E. Hansen, Local Value Capture from the Energy Transition: Insights from the Solar PV Industry in Kenya, Strathmore University, Strathmore Energy Research Centre (SERC), Kenya, 2021. Technical Report, Jun.

[34] P. Mwanzia, Factors Affecting Adoption and Scaling up of Rooftop Solar PV Deployment in Urban Centres," Master of Science Thesis, The Pan African University Institute of Water and Energy Science (PAUWES), Kenya, 2018 [Online]. Available: http://repository.pauwes-cop.net/handle/1/240.

[35] Z. Qiu, X. Zhao, P. Li, X. Zhang, S. Ali, J. Tan, Theoretical investigation of the energy performance of a novel MPCM (Microencapsulated Phase Change Material) slurry based PV/T module, Energy 87 (Jul. 2015) 686–698, https://doi.org/10.1016/j.energy.2015.05.040.

[36] A.H.A. Al-Waeli, K. Sopian, H.A. Kazem, M.T. Chaichan, Evaluation of the electrical performance of a photovoltaic thermal system using nano-enhanced paraffin and nanofluids, Case Stud. Therm. Eng. 21 (Oct. 2020), 100678, https://doi.org/10.1016/j.csite.2020.100678.

[37] Chr Lamnatou, R. Vaillon, S. Parola, D. Chemisana, Photovoltaic/thermal systems based on concentrating and non-concentrating technologies: working fluids at low, medium and high temperatures, Renew. Sustain. Energy Rev. 137 (Mar. 2021), 110625, https://doi.org/10.1016/j.rser.2020.110625.

[38] A. Alkhwaji, S. Elbahloul, M.Z. Abdullah, K.F.B.A. Bakar, Selected water thermal properties from molecular dynamics for engineering purposes, J. Mol. Liq. 324 (Feb. 2021), 114703, https://doi.org/10.1016/j.molliq.2020.114703.

[39] A.H.A. Al-Waeli, H.A. Kazem, M.T. Chaichan, K. Sopian, Photovoltaic/Thermal (PV/T) Systems: Principles, Design, and Applications, Springer International Publishing, Cham, 2019, https://doi.org/10.1007/978-3-030-27824-3.

[40] T.T. Chow, A review on photovoltaic/thermal hybrid solar technology, Appl. Energy 87 (2) (Feb. 2010) 365–379, https://doi.org/10.1016/j.apenergy.2009.06.037.
[41] P. Dupeyrat, C. Ménézo, H. Wirth, M. Rommel, Improvement of PV module optical properties for PV-thermal hybrid collector application, Sol. Energy Mater. Sol. Cells 95 (8) (Aug. 2011) 2028–2036, https://doi.org/10.1016/j.solmat.2011.04.036.
[42] K. Touafek, M. Haddadi, A. Malek, Experimental study on a new hybrid photovoltaic thermal collector, Appl. Sol. Energy 45 (3) (Sep. 2009) 181–186, https://doi.org/10.3103/S0003701X09030104.
[43] N. Aste, F. Leonforte, C. Del Pero, Design, modeling and performance monitoring of a photovoltaic–thermal (PVT) water collector, Sol. Energy 112 (Feb. 2015) 85–99, https://doi.org/10.1016/j.solener.2014.11.025.
[44] O. Rejeb, M. Sardarabadi, C. Ménézo, M. Passandideh-Fard, M.H. Dhaou, A. Jemni, Numerical and model validation of uncovered nanofluid sheet and tube type photovoltaic thermal solar system, Energy Convers. Manag. 110 (Feb. 2016) 367–377, https://doi.org/10.1016/j.enconman.2015.11.063.
[45] G. Kidegho, F. Njoka, C. Muriithi, R. Kinyua, Evaluation of thermal interface materials in mediating PV cell temperature mismatch in PV–TEG power generation, Energy Rep. 7 (Nov. 2021) 1636–1650, https://doi.org/10.1016/j.egyr.2021.03.015.
[46] M.Y. Othman, S.A. Hamid, M.A.S. Tabook, K. Sopian, M.H. Roslan, Z. Ibarahim, Performance analysis of PV/T Combi with water and air heating system: an experimental study, Renew. Energy 86 (Feb. 2016) 716–722, https://doi.org/10.1016/j.renene.2015.08.061.
[47] M.T. Chaichan, S.H. Kamel, A.-M.N.M. Al-Ajeely, in: "Thermal Conductivity Enhancement by Using Nano-Material in Phase Change Material for Latent Heat Thermal Energy Storage Systems, 5, 2015.
[48] M.E.-A. Slimani, M. Amirat, S. Bahria, Analysis of thermal and electrical performance of a solar PV/T air collector: energetic study for two configurations, in: 3rd International Conference on Control, Engineering & Information Technology (CEIT), IEEE, Tlemcen, Algeria, 2015, pp. 1–6, https://doi.org/10.1109/CEIT.2015.7232999. May 2015,.
[49] P. Dupeyrat, C. Ménézo, S. Fortuin, Study of the thermal and electrical performances of PVT solar hot water system, Energy Build. 68 (Jan. 2014) 751–755, https://doi.org/10.1016/j.enbuild.2012.09.032.
[50] S.A. Kalogirou, Y. Tripanagnostopoulos, Hybrid PV/T solar systems for domestic hot water and electricity production, Energy Convers. Manag. 47 (18–19) (Nov. 2006) 3368–3382, https://doi.org/10.1016/j.enconman.2006.01.012.
[51] N.O. Wycliffe, D.M. Mulati, D.M. Maina, Design and Characterization of a Hybrid Flat Plate Photovoltaic-Thermal System, 2016.
[52] R.M. da Silva, J.L.M. Fernandes, Hybrid photovoltaic/thermal (PV/T) solar systems simulation with Simulink/Matlab, Sol. Energy 84 (12) (2010), https://doi.org/10.1016/j.solener.2010.10.004, 1985–1996, Dec.
[53] A. Okubanjo, O. Oluwadamilola, Modelling and simulation for hybrid PV- thermal (PVT) systems for energy efficiency in Nigeria, J. Eng. Technol. 2 (1) (Jun. 2017).
[54] N. Mendalek, K. Al-Haddad, Photovoltaic system modeling and simulation, in: IEEE International Conference on Industrial Technology (ICIT), IEEE, Mar., Toronto, ON, 2017, pp. 1522–1527, https://doi.org/10.1109/ICIT.2017.7915592, 2017.
[55] S.R. Pendem, S. Mikkili, Modeling, simulation and performance analysis of solar PV array configurations (Series, Series–Parallel and Honey-Comb) to extract maximum power under Partial Shading Conditions, Energy Rep. 4 (Nov. 2018) 274–287, https://doi.org/10.1016/j.egyr.2018.03.003.
[56] N. Yıldıran, E. Tacer, Identification of photovoltaic cell single diode discrete model parameters based on datasheet values, Sol. Energy 127 (Apr. 2016) 175–183, https://doi.org/10.1016/j.solener.2016.01.024.
[57] A.A. Sfeir, Monthly average optical efficiency of flat plate collectors, Sol. Energy 30 (5) (1983) 397–399, https://doi.org/10.1016/0038-092X(83)90108-1.
[58] H.A. Zondag, W.G.J. Helden, M.J. Elswijk, M. Bakker, PV-Thermal Collector Development – an Overview of the Lessons Learnt," Presented at the 19th European PV Solar Energy Conference and Exhibition, FRANCE, PARIS, Jun. 2004.
[59] C.-Y. Huang, H.-C. Sung, K.-L. Yen, Experimental study of photovoltaic/thermal (PV/T) hybrid system, Int. J. Smart Grid Clean Energy 2 (2) (2013) 148–151, https://doi.org/10.12720/sgce.2.2.148-151.
[60] A. Ibrahim, M.Y. Othman, M.H. Ruslan, S. Mat, A. Zaharim, K. Sopian, Experimental performance analysis of solar photovoltaic thermal collector, in: Proceedings of the 9th WSEAS International Conference on System Science and Simulation in Engineering, World Scientific and Engineering Academy and Society (WSEAS), Japan, Oct. 2010, pp. 439–443.
[61] L. Kuefouet Alexis, T. Julius Kewir, D. Kanouo Boris Merlain, S. Segning Harry Bertholt, Experimental study on the electrical and thermal characteristics of a hybrid photovoltaic/thermal water solar collector model using photovoltaic solar modules of different brands, Energy Convers. Manag. X 14 (May 2022), 100198, https://doi.org/10.1016/j.ecmx.2022.100198.
[62] Z. Latt, T. Htike, Experimental performance analysis of solar photovoltaic thermal collector, IRE J. 5 (6) (Dec. 2021).
[63] M. Kamau, Firms struggle to comply with energy regulations [Online]. Available: The Standard (2021) https://www.standardmedia.co.ke/business/business/article/2001414757/firms-struggle-to-comply-with-energy-regulations.